Final Draft
of the original manuscript:

Bohlen, J.; Dobron, P.; Meza-Garcia, E.; Chmelik, F.; Lukac, P.;
Letzig, D.; Kainer, K.U.:

The Effect of Grain Size on the Deformation Behaviour of Magnesium Alloys Investigated by the Acoustic Emission Technique

In: Advanced Engineering Materials (2006) Wiley

DOI: 10.1002/adem.200600023

The Effect of Grain Size on the Deformation Behaviour of Magnesium Alloys Investigated by the Acoustic Emission Technique

Jan Bohlen[1*], Patrik Dobroň[2], Enrique Meza Garcia[1], František Chmelík[2], Pavel Lukáč[2], Dietmar Letzig[1], Karl Ulrich Kainer[1]

[1]GKSS-Forschungszentrum GmbH, Max-Planck-Str. 1, D-21502 Geesthacht, Germany

[2]Department of Metal Physics, Charles University, Ke Karlovu 5, CZ 121 16 Prague 2, Czech Republic

*corresponding author email: jan.bohlen@gkss.de

Abstract

Extruded round bars from magnesium alloys ZM21, ZK30, ZE10 and ZEK100 with various grain sizes were tested in tension and compression. The effect of grain size on the deformation behaviour of the alloys was investigated through the Hall-Petch relation. *In-situ* acoustic emission measurements were conducted during testing to evaluate the mechanisms of plastic deformation. The results are discussed with respect to twinning as one important deformation mechanism in magnesium alloys.

Introduction

Magnesium wrought alloys are developed as construction materials with a view towards light-weight applications. In this regard zinc containing magnesium alloys are of interest due to improvement of strength as reported e.g. in [1]. For contents up to 6.2 wt.% Zn occurs in solid solution [2]. Consequently, conventional alloys ZM21 and ZK30 as well as novel alloy ZE10 and its modification ZEK100 containing Zr can be tested to achieve better understanding of the influence of Zn on their deformation behaviour. Specifically, the

occurrence of a distinct deformation asymmetry, defined as the difference between the tensile and the compressive yield strength ($\Delta\sigma = \Delta\sigma_{02\ tension} - \Delta\sigma_{02\ compression} > 0$), is of interest. The asymmetry is significant in samples with a pronounced texture such as extruded bars where basal planes are mainly oriented parallel to the extrusion direction [3]. It is explained by the occurrence of the {10.2} twinning mode that contributes to the macroscopic strain only when stress is applied in tension perpendicular to the basal plane or in compression parallel to it [4]. It has been shown [5] that the deformation asymmetry depends on the grain size. This dependence can be investigated by an evaluation of parameters of the Hall-Petch relationship [6],

$$\sigma = \sigma_0 + k \cdot d^{-1/2}, \quad (1)$$

where σ_0 is the friction stress for dislocation movement and k is defined as the "Hall-Petch slope". This slope shows a dependence on the misorientation of the neighbouring grains as well as on the critical resolved shear stresses for the activated slip modes in them. Equation (1) describes also the influence of grain size on deformation twinning in Mg alloys containing Al [5].

Acoustic emission (AE) stems from transient elastic waves generated within the material due to sudden irreversible structural changes such as dislocation motion and twinning. It yields therefore information on their role during deformation.

In the present work results of *in-situ* AE measurements during tensile and compression testing are used to investigate the effect of grain size on the deformation asymmetry in Mg alloys containing Zn as the main alloying element.

Experimental

Cast billets from Mg alloys ZM21, ZK30, ZE10 and ZEK100 (see Tab. 1 for the composition) were used for this study. Round bars were extruded using indirect or hydrostatic procedure with a variation of process parameters to achieve different grain sizes. Details about these

extrusion trials can be found e.g. in [7, 8]. Samples for tensile tests were machined to a diameter of 6 mm and the gauge length of 30 mm. Samples for compression tests had a diameter of 10 mm and the length of 15 mm.

A universal testing machine (Zwick Z050) was used for both, tensile and compression tests. Tests were performed at room temperature and at a constant strain rate of 10^{-3} s^{-1}. The yield strength $\sigma_{0.2}$ was taken as 0.2% proof stress or as the lower elastic limit σ_{low}, where applicable. The microstructure was investigated on longitudinal sections of the bars using light microscopy [9]. The average grain size was determined from the micrographs by computer-aided linear intercept measurements.

The computer controlled DAKEL-XEDO-3 AE system was used to monitor AE through the two-threshold-level detection procedure [10]. A miniaturized MST8S piezoelectric transducer (diameter of 3 mm) was attached on the tensile specimen surface with the help of silicon grease and a spring. In case of compression tests a waveguide was attached to one of the dies which were in direct contact to the sample and the transducer was used. The total gain was of 90 dB in both cases. It should be noted that beside of the different setup also the tensile and compression samples had different volumes. Therefore, the AE parameters from tensile and compression tests cannot be compared directly. Details about the parameter settings during detection can be found in [5].

Results

Figs. 1 a-d show typical micrographs of the studied alloys. For ZM21 (Fig. 1a), a homogeneously recrystallised microstructure containing homogeneously distributed small precipitates as well as some twins. In ZK30 (Fig. 1b) as well as in ZE10 (Fig. 1c) the formation of new grains after extrusion is apparent. However, the recrystallisation process is obviously not completed. For ZEK100 (Fig. 1d) a slightly better homogeneity of the grain structure is observed.

The average grain size is correlated with the yield strength from tension and compression tests in a Hall-Petch plot for ZM21 in Fig. 2 and for ZK30 in Fig. 3. For ZM21 a least-square fit was used for the evaluation of the parameters of the Hall-Petch relation. In case of the ZK30 alloy only the slopes of best-fitted guidelines are shown because of the larger scatter of the data. The curve slopes are steeper in compression than in tension for both alloys. They are also steeper for ZK30 than for ZM21 in both testing modes. Fig. 3 also includes results for ZE10 and ZEK100. It is interesting that the behaviour of these two alloys is similar like that of ZK30. Fig. 4 summarizes data on the yield asymmetry $\Delta\sigma$ for all alloys. The drawn dependences were taken from the analysis in Figs. 2 and 3. It can be seen that the yield asymmetry decreases with decreasing grain size for ZM21 and ZK30. Furthermore, the asymmetry is lower for ZM21 than for ZK30. ZE10 and ZEK100 show asymmetry values comparable with those for ZK30.

Stress-strain curves from tensile tests correlated with the AE count rates at two thresholds N_{c1} and N_{c2} (total count rate and burst count rate, respectively) as functions of the test time are shown in Figs. 5 a-d. The count rates increase with testing time to a peak maximum which corresponds to the macroscopic yield point, then they decrease first by a sudden drop followed by a further slower decrease lasting till the fracture of the sample. In order to evaluate the cumulative AE activity as a function of the alloy composition the total count numbers detected throughout the measurement are also indicated in Figs. 5 a-d. The count numbers decrease with increasing content of Zn. The count numbers in ZEK100 are significantly higher than in the other alloys.

The results for the compression tests are shown in Figs. 6 a-d. The AE count rates show again a peak at the beginning of the plastic flow. However, this peak is not sharp as its width is much greater compared to those from tension tests, persisting up to 4 – 5 % of strain. Subsequently, a significant drop of the count rates is seen, especially for the burst rate N_{c2}. Interestingly, the number of counts (cumulative AE activity) does not show significant

differences if the four alloys of this study were compared. This is different than for the AE activity during tensile testing,

The AE count rates decrease with decreasing grain size during tensile as well as during compression testing. This is in agreement with observations for other Mg alloys [11].

Discussion

As the Zn-contents in all investigated alloys is lower than the solid solubility limit of 6.2 wt.% in pure Mg [2], precipitates observed in ZE10 and ZEK100 are a consequence of a very low solubility of rare earth elements and Zr. However, the microstructure contains only a small amount of precipitates or particles. Zr addition in the ZE100 alloy leads apparently to a more homogeneous microstructure (Fig. 1d). A clearly recrystallised microstructure is obtained only for ZM21. Fine precipitates distributed within the grains can be observed in this alloy due to the addition of Mn [12].

The influence of the grain size on the deformation behaviour of ZM21 and ZK30 may be deduced from Figs. 2 and 3. Due to the textured samples and the dependence of the Hall-Petch slope k on misorientation of neighbouring grains we cannot state on "true" Hall-Petch parameters. This is also reflected in the fact that different values of these parameters are obtained in tension and in compression. However, this aspect allows us to analyse deformation mechanisms by analysing the slopes calculated from our data. For both alloys a significant increase of the yield strength with decreasing grain size is observed in tension and compression. This effect is more pronounced in ZK30 which corresponds with higher yield strength in both testing modes. For both alloys the slopes are higher in compression than in tension. This observation can be explained by the fact that {10.2} twinning is geometrically more favoured in compression than in tension and that the activity of twinning decreases with decreasing grain size. Due to this fact the yield asymmetry should also disappear in grain refined material, as has been observed (Fig. 4). The asymmetry is generally higher for ZK30

than for ZM21. The values of ZE10 and ZEK100 are more comparable to those of ZK30 than to those of ZM21.

Akthar and Teghtsoonian [13] reported that the addition of zinc reduces the critical resolved shear stress for prismatic slip. It is also likely that the critical resolved shear stress of <c+a> pyramidal slip is reduced with addition of an alloying element such as zinc (both are of non-basal type). This might reduce the tendency to twinning. The AE results in compression tests show no significant difference in the twinning activity in ZE10, ZEK100 and ZK30. Note, that twinning contributes to the macroscopic strain along the c-axis of the hexagonal lattice cell. Also <c+a> pyramidal slip contributes in a certain extent whereas prismatic slip does not. So the effect of easier activation of the prismatic slip most probably does not influence the activity of twinning [14]. The ZM21 alloy is the only one with an apparent decrease in the yield asymmetry. This may indicate that this decrease is not a single effect of the Zn addition but also may be connected with the addition of Mn, either in solid solution or in precipitates.

The AE response during tensile testing (Fig. 5) is similar for all investigated alloys. The AE peak at the yield point may be explained by collective dislocation motion and twinning, the subsequent drop in the count rates is well understood by the beginning of strain hardening in these materials where dislocation motion is hindered by forest dislocations. Although twinning is not favoured in tension we still observe significant count rates till the fracture of the sample. Assuming that for polycrystals with a relatively high elongation to fracture (more than 20%) the von Mises criterion of compatibility (necessarity of five independent slip systems [15]) has to be fulfilled it is obvious that twinning contributes to the macroscopic strain. This would be in accordance with the AE count rates persisting up to high strains.

The AE results for compression somewhat differ from those for tension. The AE peak that corresponds to the yield point is broader and persists up to 4 –5 % of strain. Furthermore, it consists mainly of burst type signals. This observation is in accordance with the conclusion that twinning plays a more important role during compression. In the subsequent stages of

deformation no burst type signals are observed anymore and the continuous emission becomes very weak with increasing strain. This is in agreement with a strain hardening, which is much more pronounced in compression than in tension (this becomes simply visible if the maximum stress is compared to the yield strength). It can be anticipated that twinning does not occur if no burst type emission is observed because twinning is an excellent source of AE. This corresponds well with results of Davies et al. [16], who observe an almost complete re-orientation of the sample in *in-situ* texture measurements during compression testing. This is attributed to twinning within the first 6% of strain.

Above conclusion is qualitatively the same for all alloys of this study. However, there are some differences in the observed count rates. The cumulative AE activity in Fig. 5 show a significant decrease for tensile tests if the Zn content increases. Only the ZEK100 alloy does not fit into this scheme. On the other hand, there is no such significant difference in compression (Figs. 6). The decrease of the count number can generally be explained by solid solution strengthening as reported by Kleiner and Uggowitzer for AZ alloys [17].

During compression, the strain hardening effect occurs due to twinning itself and obviously is not much affected by the addition of Zn. This appears as a nearly constant count number with increasing content of Zn. This conclusion is not surprising for ZE10 and ZK30, but ZM21, which showed a somewhat lower yield asymmetry, is also not affected. In fact it means that a lower yield asymmetry does not indicate a decrease in the twinning activity throughout straining. This effect may be due to additional strengthening by Mn in solid solution and/or in precipitates.

Conclusion

The influence of grain size on the deformation of the Mg alloys ZE10, ZEK100, ZM21 and ZK30 was investigated by the acoustic emission technique. A deformation asymmetry (difference of tensile and compression yield stresses) has been found in all these alloys. This

asymmetry decreases with decreasing grain size and, somewhat also with increasing content of solute elements like Mn. It is suggested that the decrease of asymmetry with decreasing grain size may be explained by reduced twinning activity. On contrary, the increasing solute content seems to influence the alloy hardening. The influence on twinning activity is rather minor.

Acknowledgements

It is the authors pleasure to dedicate this paper on the occasion of the 50th anniversary of GKSS Research Centre in Geesthacht / Germany. The authors appreciate support by Dipl.-Ing. Jacek Swiostek (GKSS) and Dr. Hans-Ulrich Menzel (CEP GmbH Freiberg) during hydrostatic extrusion trials. Also support by Dipl.-Ing. Sören Müller (TU Berlin) during indirect extrusion trials as part of the “Virtual Institute – Key materials for light weight contruction” is appreciated. Financial support by the Hermann von Helmholtz Association (HGF) is acknowledged. This work is also a part of the Research Project 1M 2560471601 "Eco-centre for Applied Research of Non-ferrous Metals" that is granted by the Ministry of Education, Youth and Sports of the Czech Republic.

References

[1] Aluminium-Zentrale Düsseldorf: Magnesium Taschenbuch, 1. Auflage, Aluminium-Verlag Düsseldorf, Deutschland, 2000.

[2] T. B. Massalski, J. L. Murray, L.H. Bennett (Ed.), Binary Alloy Phase Diagrams, American Socity for Metals, Metals Park, 1987.

[3] I. L. Dillamore, W.T. Roberts, Metall. Rev. 10 (1965) 271.

[4] P. G. Partridge, Metall. Rev. 118 (1967) 169.

[5] J. Bohlen, P. Dobron, J. Swiostek, D. Letzig, F. Chmelik, P. Lukac, K. U. Kainer, Mat. Sci. Eng. A (2006), (Proceedings of ISPMA 10), *submitted*.

[6] P. Haasen: Physical Metallurgy, Cambridge University Press, Cambridge, 1996.

[7] J. Swiostek, J. Bohlen, D. Letzig, K. U. Kainer, Mat. Sci. Forum 488 – 489 (2005) 491.

[8] J. Swiostek, D. Letzig, K. U. Kainer, Proceedings of the First Russian International Conference and Exhibition of Magnesium – Broad Horizons, Nov 29th – Dec 01st 2005, submitted.

[9] V. Kree, J. Bohlen, D. Letzig, K.U. Kainer, Pract. Metallography 41 (2004) 233.

[10] Standard Practice for Acoustic Emission Examination of Fiberglass Reinforced Plastic Resin, ASTM E 1067-85. Tank/Vessels, May 31, 1985.

[11] P. Dobroň, J. Bohlen, F. Chmelík, D. Letzig, K. U. Kainer: Acoustic Emission Analysis of Extruded AZ31 with Varying Grain Size, Kovove Mat. 43 (2005) 192.

[12] ASM Specialty Handbook: Magnesium and Magnesium Alloys (Eds. M.M. Avedesian, H. Baker), ASM International, 1999

[13] A. Akthar, E. Teghtsoonian, Phil. Mag. 25 (1972) 897.

[14] G. Mann, J. R. Griffiths, C. H. Caceres, J. Alloys Comp. 378 (2004) 188.

[15] R. von Mises, Z. Angew. Math. Mech., 8 (1928) 161.

[16] C. H. J. Davies, S. Yi, J. Bohlen, K. U. Kainer, H.-G. Brokmeier, Mat. Sci. Forum 495 – 497 (2005) 1633.

[17] S. Kleiner, P. J. Uggowitzer, Mat. Sci. Eng. A 379 (2004) 258.

Table 1: Composition of the used materials (all data in wt.%)

Alloy	Zn	Mn	Rare Earth Elements (SE)	Zr	Mg
ZM21	2.1	0.75	–	–	balance
ZE10	1.4	–	0.2	–	balance
ZK30	3.2	<0.03	–	0.55	balance
ZEK100	1.4	–	0.2	0.6	balance

Figures

Fig. 1: Micrographs from longitudinal sections of extruded bars of a) ZM21, b) ZK30, c) ZE10, d) ZEK100, extrusion direction horizontal

Fig. 2: Tensile and compressive yield strength *vs*. inverse square root of average grain size for extruded bars from ZM21.

Fig. 3: Tensile and compressive yield strength *vs*. inverse square root of average grain size for extruded bars of ZK30, ZE10 and ZEK100.

Fig. 4: Tensile/compression asymmetry *vs*. inverse square root of the average grain size for extruded round bars (guidelines for the eyes stem from Hall-Petch analysis).

Fig. 5: Stress strain curve correlated with AE count rates $\dot{N}_{C1}$ and $\dot{N}_{C2}$ from a tensile test of an extruded bar, a) ZM21 (average grain size 12 µm), b) ZK30 (average grain size 13 µm), c) ZE10 (average grain size 13 µm), d) ZEK100 (average grain size 16 µm)

Fig. 6: Same as Fig. 5 but for compression tests, a) ZM21, b) ZK30, c) ZE10, d) ZEK100

Figures

a) b)

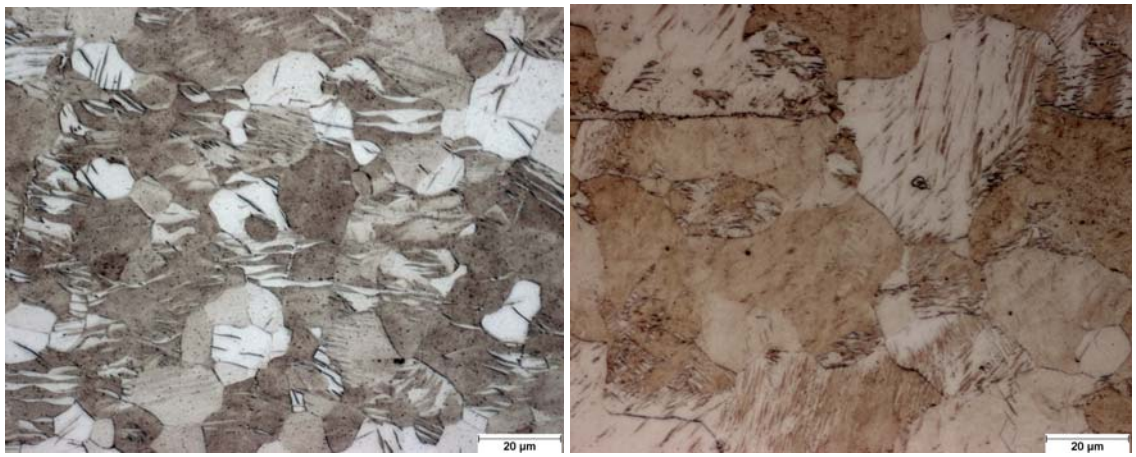

c) d)

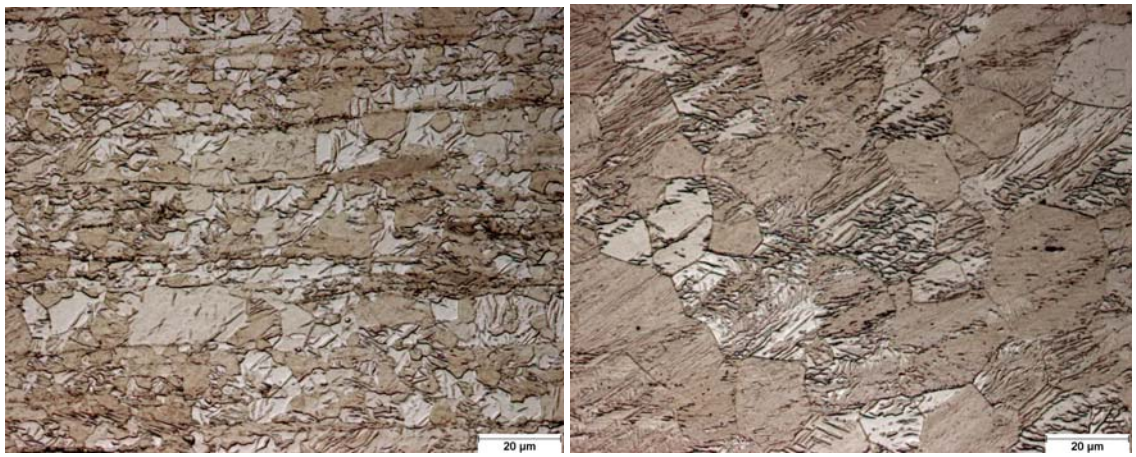

Fig. 1: Micrographs from longitudinal sections of extruded bars a) ZM21, b) ZK30, c) ZE10, d) ZEK100, extrusion direction horizontal

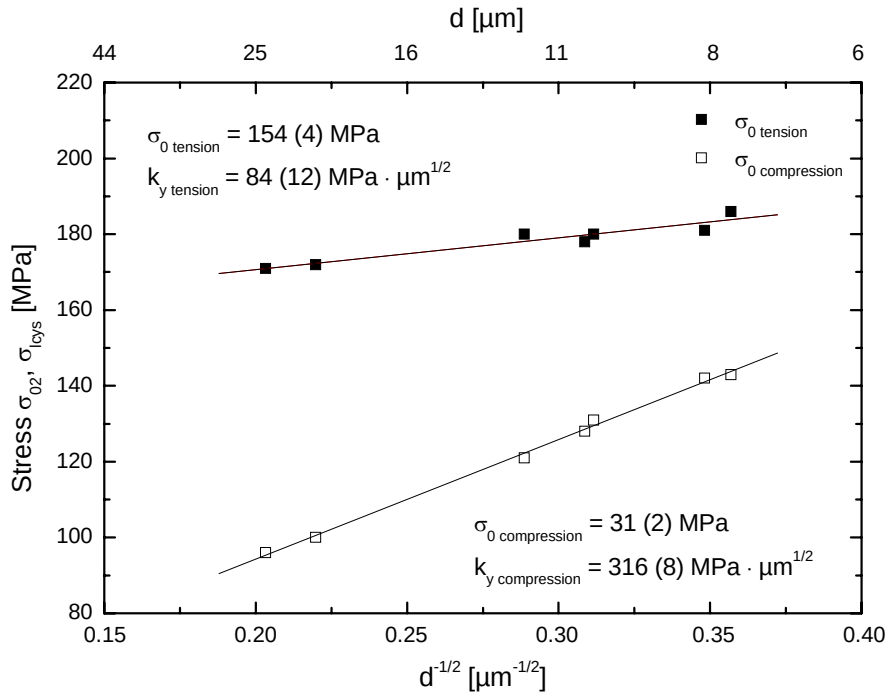

Fig. 2: Tensile and compressive yield strength *vs.* inverse square root of average grain size for extruded bars from ZM21

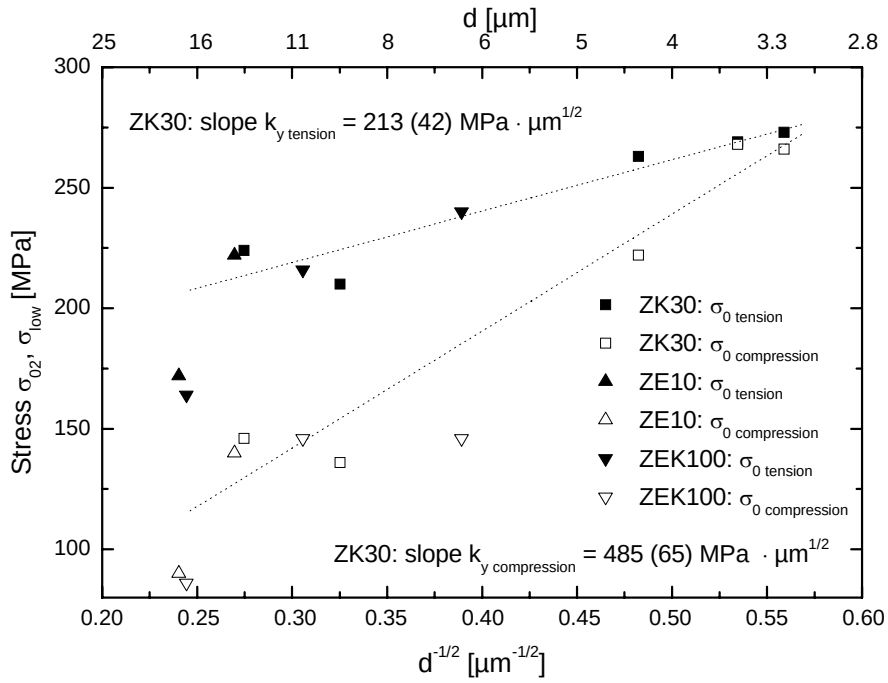

Fig. 3: Tensile and compressive yield strength *vs*. inverse square root of average grain size for extruded bars from ZK30 including also data from ZE10 and ZEK100

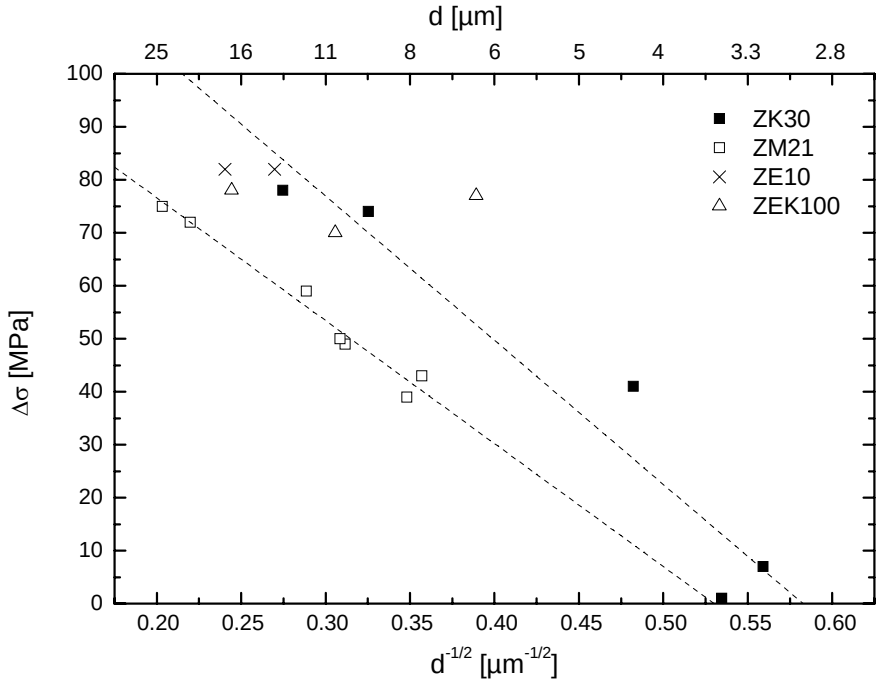

Fig. 4: Tensile/Compression asymmetry *vs.* inverse square root of the average grain size for extruded round bars (guidelines for the eyes stem from Hall-Petch analysis)

a) b)

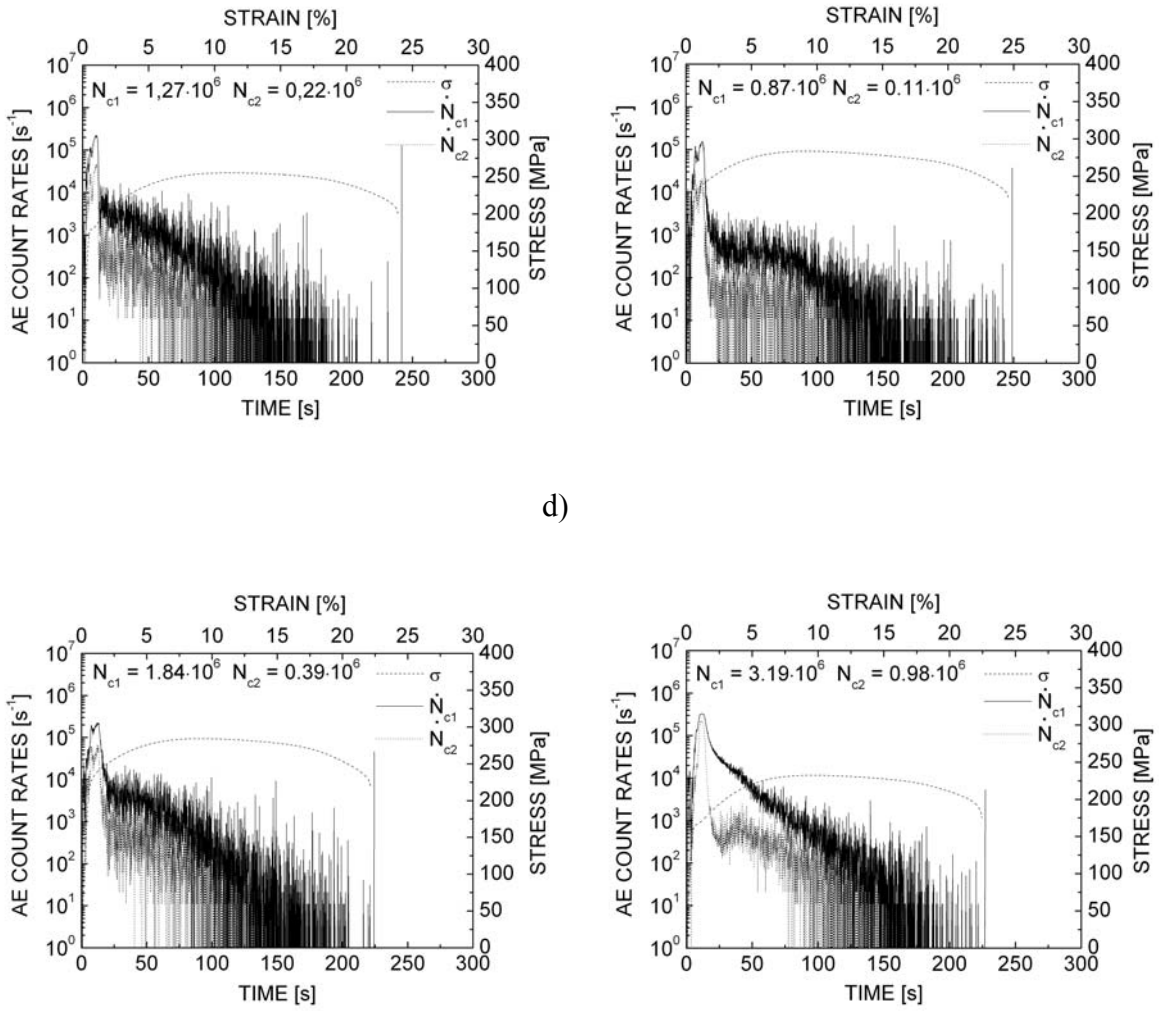

c) d)

Fig. 5: Stress strain curve correlated with AE count rates $\dot{N}_{C1}$ and $\dot{N}_{C2}$ from a tensile test of an extruded bar, a) ZM21 (average grain size 12 µm), b) ZK30 (average grain size 13 µm), c) ZE10 (average grain size 13 µm), d) ZEK100 (average grain size 16 µm)

a) b)

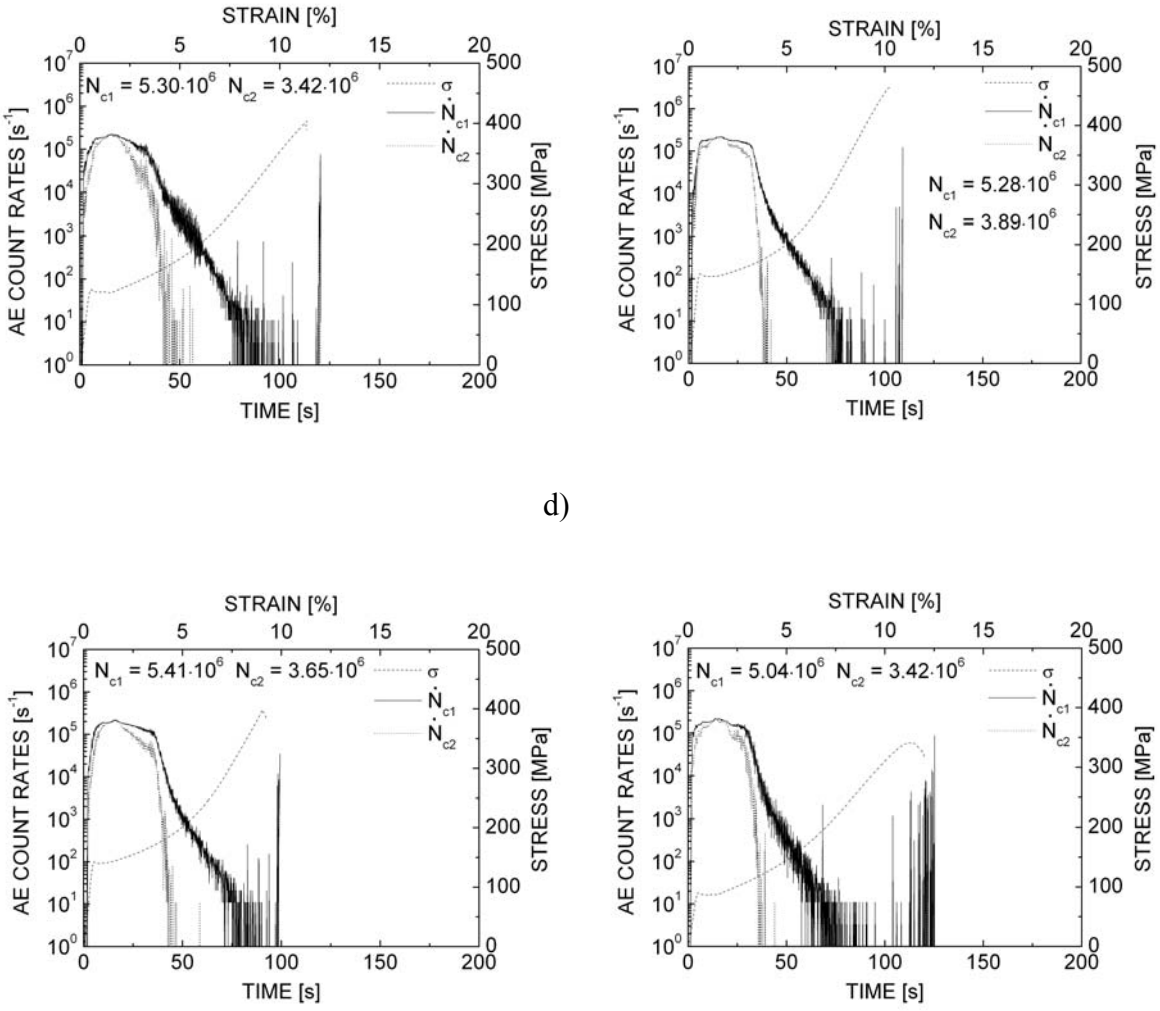

c) d)

Fig. 6: Same as Fig. 5 but for compression tests, a) ZM21, b) ZK30, c) ZE10, d) ZEK100